



Short communication

## 3D graphene aerogel anchored tungstophosphoric acid catalysts: Characterization and catalytic performance for levulinic acid esterification with ethanol

Min Wu<sup>a</sup>, Xiaoli Zhang<sup>a</sup>, Xiaoli Su<sup>a</sup>, Xueyang Li<sup>a</sup>, Xiucheng Zheng<sup>a,b,\*</sup>, Xinxin Guan<sup>a</sup>, Pu Liu<sup>a</sup><sup>a</sup> College of Chemistry and Molecular Engineering, Zhengzhou University, Zhengzhou 450001, China<sup>b</sup> Key Laboratory of Advanced Energy Materials Chemistry (Ministry of Education), Nankai University, Tianjin 300071, China

## ARTICLE INFO

## Article history:

Received 26 April 2016

Received in revised form 23 June 2016

Accepted 24 July 2016

Available online 27 July 2016

## Keywords:

GA

HPW/GA

Esterification

Levulinic acid

Biofuel

## ABSTRACT

3D graphene aerogel (GA) was synthesized from graphene oxide (GO) using a hydrothermal procedure combined with freeze-drying. Then, they were used to assemble the supported  $H_3PW_{12}O_{40}$  (HPW) catalysts. The optimization of the reaction parameters for levulinic acid esterification with ethanol was performed and the catalytic performance of the HPW/GA catalysts was comparatively investigated. The results showed that these catalysts had abundant porous structure. In particular, they were found to be efficient in the synthesis of ethyl levulinate, which is promising in reducing the consumption of petroleum-derived fossil fuels.

© 2016 Elsevier B.V. All rights reserved.

## 1. Introduction

As an alternative renewable energy resource, biofuel has attracted considerable attention to meet the increasing demands for energy and the growing level of greenhouse gases [1–4]. In particular, ethyl levulinate is an excellent diesel miscible biofuel since it can be used up to 5 wt% directly in regular diesel engines [5]. The conventional catalysts for levulinic acid (LA) esterification are mineral acids such as HCl,  $H_2SO_4$  and  $H_3PO_4$ . Unfortunately, due to their un-recyclability, harsh reaction conditions and operational problems, replacement of those homogeneous catalysts by the heterogeneous ones is highly desirable [6]. On the other hand, 12-tungstophosphoric acid (HPW) with Keggin structure has been widely used because of its strong acid and good redox properties. However, the high solubility in polar solvents, low thermal stability and low surface area restrict its application as a solid acid catalyst. Supporting or encapsulating HPW species with strong dispersion on or in a suitable carrier with high surface area, which is insoluble in the reaction media, could overcome these limitations [7,8]. The dispersion on or in the carriers may increase the active sites of HPW species and the interaction between HPW and carriers may restrain the leaching of HPW from the resultant heterogeneous catalysts. This could improve the catalytic activity and stability of HPW.

As one of the most prevailing 3D macroscopic architectures of graphene, graphene aerogel (GA) exhibits intriguing features such as high porosity, large specific surface area, and high electrical conductivity. Therefore, GA provides exceptional potential in a variety of sustainable applications including catalysis [9,10]. Even so, no work has been reported on the application of GA in esterification reaction.

In the present work, GA was hydrothermally assembled and used as supports to prepare HPW-based catalysts. The optimization of the reaction conditions for LA esterification with ethanol was performed and the catalytic performance of the resultant HPW/GA catalysts for the esterification of LA was systematically investigated.

## 2. Experimental methods

GA was prepared from graphene oxide with a hydrothermal method combined with freeze-drying [11] and HPW was synthesized with an improved diethyl ether extraction method [12]. HPW/GA catalysts were prepared by using an impregnation technique similar to that of HSiW/MCM-41 [13] and the resultant catalysts were denoted as  $x$  wt% HPW/GA ( $x = 5, 10, 15, 20, 25, 30, 35, 40,$  and  $45$ , respectively).

The samples were characterized by X-ray diffraction (XRD), nitrogen adsorption-desorption isotherms, scanning electron microscopy (SEM), transmission electron microscopy (TEM), Fourier-Transform infrared spectroscopy (FT-IR), and nitrogen adsorption-desorption isotherms.

The catalytic performance of the resultant catalysts for the esterification of LA with ethanol was done in a round-bottom flask equipped with

\* Corresponding author at: College of Chemistry and Molecular Engineering, Zhengzhou University, Zhengzhou 450001, China.  
E-mail address: [zhxch@zzu.edu.cn](mailto:zhxch@zzu.edu.cn) (X. Zheng).

a magnetic stirrer and a water-cooled condenser. The products were analyzed by a gas chromatograph (GC2010 II) equipped with an OV-1701 capillary column (30 m × 0.53 mm × 0.33 μm) and a FID detector. 45 wt% HPW/GA was repeatedly used to examine the recyclability of the resultant catalysts. After each catalytic run, the catalysts were recovered from the reaction solution by centrifugation, washed with ethanol and dried at 70 °C.

The detailed information about this section was supplied in the “Electronic Supplementary Material”.

### 3. Results and discussion

The XRD patterns shown in Fig. 1 reveal that only the characteristic phase of GA exists in the resultant *x* wt% HPW/GA catalysts when *x* is less than 10, suggesting that the HPW species are well dispersed. The characteristic peaks of HPW appear when *x* is greater than or equal to 10 and the intensity increases with increasing HPW loading. The slight change of the crystalline structure in the HPW/GA catalysts perhaps is caused by the interaction of the oxygen-containing groups in GA and HPW, which may affect the secondary structure of tungstophosphoric acid.

One can see from Fig. 2 that the N<sub>2</sub> adsorption-desorption isotherms for the HPW/GA catalysts are similar to that of GA, indicating these catalysts retain the textural structure of GA. The loading of HPW significantly affects the textural parameters. As expected, both the specific surface area and pore volume relative to those of GA ( $S_{\text{BET}} = 270.1 \text{ m}^2 \text{ g}^{-1}$ ,  $V_p = 0.2111 \text{ cm}^3 \text{ g}^{-1}$ ) decrease with increasing HPW loading. This could be attributed to the deposition of HPW species inside the pores or dispersion of them on the surfaces of GA. Even so, the HPW/GA catalysts display much higher textural parameters than that of the pristine HPW ( $S_{\text{BET}} = 5.4 \text{ m}^2 \text{ g}^{-1}$ ,  $V_p = 0.0103 \text{ cm}^3 \text{ g}^{-1}$ ), which is attributed to the contribution of GA (Table 1). For instance, the pore volume and surface area for 45 wt% HPW/GA are  $0.0878 \text{ cm}^3 \text{ g}^{-1}$  and  $123.1 \text{ m}^2 \text{ g}^{-1}$ , respectively. The unique properties would be helpful for increasing their catalytic activities. Meanwhile, the various loadings of HPW have no much effect on the pore size. This may be explained that part of HPW species block the microspores or are encapsulated in the macropore of GA since these pores could not be detected by the BJH method.

As shown in Fig. S1, the FT-IR spectrum of 5 wt% HPW/GA catalysts only exhibits the characteristic IR bands of GA. The characteristic bands of HPW, such as the asymmetry vibrations of P—O<sub>a</sub> (internal oxygen connecting P and W,  $1082 \text{ cm}^{-1}$ ), W—O<sub>d</sub> (terminal oxygen bonding to W atom,  $983 \text{ cm}^{-1}$ ), W—O<sub>b</sub>—W (edge-sharing oxygen connecting W,  $890 \text{ cm}^{-1}$ ) and W—O<sub>c</sub>—W (corner-sharing oxygen connecting W<sub>3</sub>O<sub>13</sub> units,  $804 \text{ cm}^{-1}$ ) [12], disappear in the catalysts. This is ascribed to the dilution of GA. These bands appear in the case

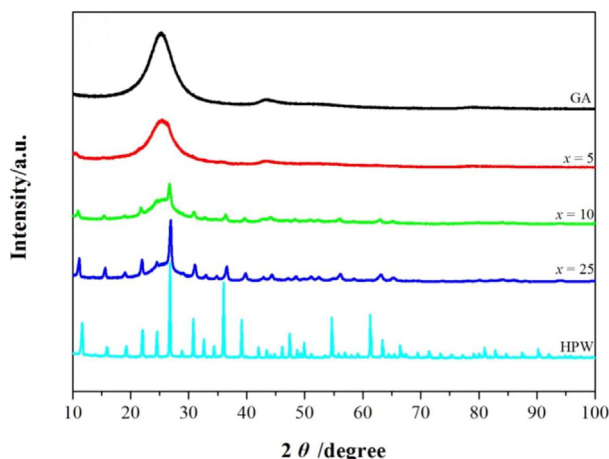


Fig. 1. XRD patterns of GA, HPW, and the *x* wt% HPW/GA catalysts.

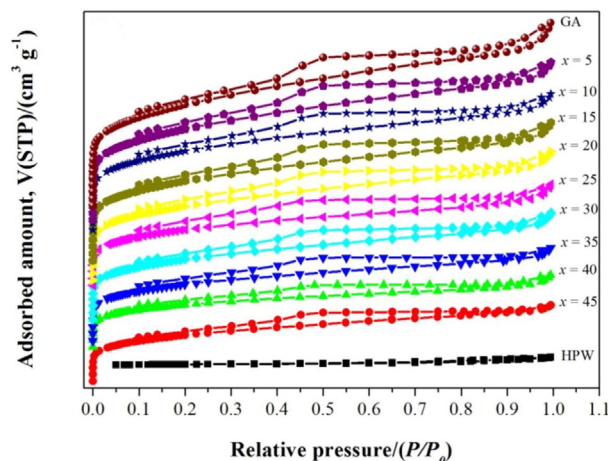


Fig. 2. N<sub>2</sub> adsorption-desorption isotherms of GA, HPW, and the *x* wt% HPW/GA catalysts.

of 25 wt% HPW/GA catalysts and the absorbance gradually increases with increasing HPW loading, which could be used to identify the existence of Keggin phase in the resultant catalysts.

The morphology and structure of the 15 wt% HPW/GA catalysts are characterized by SEM and TEM techniques (Fig. S2). As shown in Fig. S2a, the catalysts retain the well-defined and interconnected 3D porous network of GA, which is caused by the partial overlapping or coalescing of graphene sheets and macroporous architectures [15]. Meanwhile, the HPW particles are anchored uniformly on or wrapped by graphene sheets. This is also confirmed by the TEM images with different magnifications shown in Fig. S2c and d.

Ethanol-to-LA molar ratio ( $n_{\text{ethanol}}/n_{\text{LA}}$ ) and reaction temperature are optimized to maximize LA conversion which is esterified with ethanol over 15 wt% HPW/GA catalysts. The value of  $n_{\text{ethanol}}/n_{\text{LA}}$  is varied in the range of 1.0–15.0 and their influences are depicted in Fig. 3a. LA conversion is found to increase from 8.3% to 35.0% with increasing  $n_{\text{ethanol}}/n_{\text{LA}}$  from 1.0 to 10.0 since the esterification reaction is reversible and the excess amount of ethanol used may favor the conversion of LA to some extent. However, the conversion value decreases when  $n_{\text{ethanol}}/n_{\text{LA}}$  is further increased. This is may be ascribed to the decrease the contact opportunities for LA species with the catalysts due to the dilution of too much ethanol. Thus,  $n_{\text{ethanol}}/n_{\text{LA}}$  is optimized to be 10.0 under the reaction conditions. As shown in Fig. 3b, the LA conversion increases with increasing reaction time and changes from 5.8% after 2 h to 18.0% after 9 h. When the reaction time is further increased to 10 h, the value only increases to 18.1%. Thus, 9 h is an optimum reaction time under the present conditions. Fig. 3c shows the catalytic activities of the resultant *x* wt% HPW/GA catalysts. It is found that the LA conversion increases with increasing HPW loading. The value drastically increases from 11.2% to 89.1% when *x* increases from 5 to 45, which is consistent with that of the Keggin-anion density (Table 1). On the other hand, in order to reflect actual catalytic performance of HPW species in the resultant catalysts, their activities are also compared with the TOF mode. As shown in the inset of Fig. 3c, although the LA conversion and the Keggin-anion density are the lowest for 5 wt% HPW/GA ascribed to the lowest HPW loading and the highest surface area, it exhibits the highest TOF value ( $0.031 \text{ mol}_{\text{LA}} \cdot \text{h}^{-1} \cdot \text{g}_{\text{HPW}}^{-1}$ ) among the resultant catalysts. As for 35 wt% HPW/GA catalysts, the LA conversion (70.3%) is higher than the ones with low loadings ( $x = 5\text{--}30$ ) and TOF value ( $0.028 \text{ mol}_{\text{LA}} \cdot \text{h}^{-1} \cdot \text{g}_{\text{HPW}}^{-1}$ ) is similar or even higher than the ones with high loadings ( $x = 40, 45$ ). Therefore, the optimized loading for HPW on GA is 35 wt% under the present conditions.

In order to investigate the durability of these HPW/GA catalysts, a typical recycle study on the sample with 45 wt% HPW loading is performed, as shown in Fig. 3d. The LA conversion decreases from 89.1% to 76.6% in the second cycle. Comparing with that of the fresh one, the

# دانلود مقاله



<http://daneshyari.com/article/49243>



- ✓ امکان دانلود نسخه تمام متن مقالات انگلیسی
- ✓ امکان دانلود نسخه ترجمه شده مقالات
- ✓ پذیرش سفارش ترجمه تخصصی
- ✓ امکان جستجو در آرشیو جامعی از صدها موضوع و هزاران مقاله
- ✓ امکان پرداخت اینترنتی با کلیه کارت های عضو شتاب
- ✓ دانلود فوری مقاله پس از پرداخت آنلاین
- ✓ پشتیبانی کامل خرید با بهره مندی از سیستم هوشمند رهگیری سفارشات